Topographical and nanomechanical characterization of casein nanogel particles using atomic force microscopy

Asma Bahri, Marta Martin, Csilla Gergely, Sylvie Marchesseau, Dominique Chevalier-Lucia

Accepted Manuscript

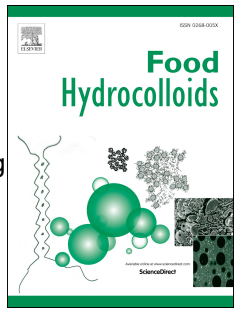

Topographical and nanomechanical characterization of casein nanogel particles using atomic force microscopy

Asma Bahri, Marta Martin, Csilla Gergely, Sylvie Marchesseau, Dominique Chevalier-Lucia

PII: S0268-005X(17)32061-1

DOI: 10.1016/j.foodhyd.2018.03.029

Reference: FOOHYD 4340

To appear in: *Food Hydrocolloids*

Received Date: 13 December 2017

Revised Date: 14 March 2018

Accepted Date: 14 March 2018

Please cite this article as: Bahri, A., Martin, M., Gergely, C., Marchesseau, S., Chevalier-Lucia, D., Topographical and nanomechanical characterization of casein nanogel particles using atomic force microscopy, *Food Hydrocolloids* (2018), doi: 10.1016/j.foodhyd.2018.03.029.

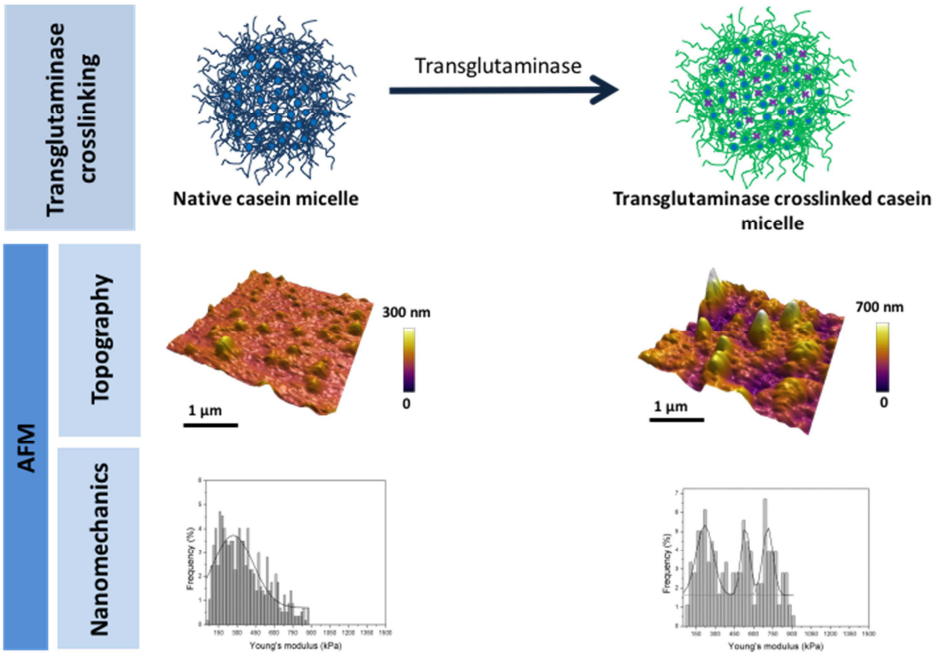

Comment citer ce document :
Bahri, A., Martin, M., Gergely, Marchesseau, S., Chevalier-Lucia, D. (2018). Topographical and nanomechanical characterization of casein nanogel particles using atomic force microscopy. Food Hydrocolloids, 83, 53-60. , DOI : 10.1016/j.foodhyd.2018.03.029

Topographical and nanomechanical characterization of casein nanogel particles using atomic force microscopy

Asma Bahri[a], Marta Martin[b], Csilla Gergely[b], Sylvie Marchesseau[a], Dominique Chevalier-Lucia[a*]

[a] IATE, Université de Montpellier, CIRAD, INRA, Montpellier SupAgro, Montpellier, France

[b] L2C, Université de Montpellier, CNRS, Montpellier, France

[*]Corresponding author:

dominique.chevalier-lucia@umontpellier.fr

Université de Montpellier

CC023 – UMR IATE

Place Eugène Bataillon

34095 Montpellier cedex 5 - France

Abstract

Casein micelle (CM), porous colloidal phosphoprotein-mineral complex, naturally present in milk to deliver minerals, also has several features, which could ensure its use as nanocarrier for bioactives. CM structure being not steady according to the physico-chemical conditions, its stability can be improved by intra-micellar cross-linking using transglutaminase (TGase) inducing a strengthened structure called casein nanogel. The aim of this research was to investigate the morphology and nanomechanics of casein nanogel particles cross-linked by TGase (TG-CM) using atomic force microscopy (AFM) in native-like liquid environment (lactose-free simulated milk ultrafiltrate, SMUF). Prior to AFM, TG-CM were captured by anti-phospho-Ser/Thr/Tyr monoclonal antibodies covalently bound to a gold-coated slide via

carbodiimide chemistry. Surface topography and size properties evaluation revealed an increase in size of TG-CM compared to native CM, TG-CM being characterized by a mean width of 264 ± 7 nm and a mean height of 111 ± 5 nm. TG-CM displayed a relatively high contact angle (62°) indicating a limited flattening of these particles after adsorption on the substrate. The TG-CM elasticity was then evaluated applying low indentation forces on single TG-CM. The TGase treatment led to a significant modification of CM nanomechanics attributed to intramolecular rearrangements within the micellar structure. The elasticity distribution of TG-CM revealed three elasticity peaks centered at 219 ± 14 kPa, 536 ± 14 kPa and 711 ± 11 kPa. The lower elasticity peak is related to the native CM elasticity characteristic and the two stiffer peaks were attributed to the substantial changes in the TG-CM structure.

Keywords: Casein micelle; Nanogel; Transglutaminase; Atomic force microscopy; Topography; Nanomechanics

1. Introduction

With the growing awareness of food importance on disease prevention and cure, novel strategies have been developed to include and deliver bioactive compounds through food matrices (Katouzian & Jaffary, 2016; Prakash & van Boekel, 2010; Zhu, 2017). Particularly, nanoencapsulation of bioactives has been proposed to protect them against degradation during processing, increase their bioavailability and monitor their release to the desired site after ingestion (Katouzian & Jaffary, 2016). Casein micelles (CM) are natural polymeric nanocarriers for delivery of minerals, particularly calcium and phosphate (de Kruif & Holt, 2003). Consequently, bioactives delivery systems have been developed from nanosized native CM or modified CM (Chevalier-Lucia, Blayo, Gracià-Julià, Picart-Palmade, & Dumay, 2011; Livney, 2010; Ranadheera, Liyanaarachchi, Chandrapala, Dissanayake, & Vasiljevic, 2016). CM is a naturally self-assembly of caseins, major milk proteins (~ 80%), through hydrophobic bonds and colloidal calcium phosphate bridges. The main four caseins α_{s1}, α_{s2}, β and κ are phosphoproteins present at a molar ratio of ~4:1:4:1.6 in CM (Walstra, Geurts, Noomen, Jellema, & van Boekel, 1999). CM has a hydrodynamic diameter of ~200 nm and a highly hydrated structure retaining ~3.7 g water/g of dry casein (McMahon & Brown, 1984). It is characterized by a hydrophobic core and a hydrophilic shell, CM surface being covered by a κ-casein brush insuring its stability thanks to electrostatic and steric repulsion (Dalgleish, Horne, & Law, 1989; De Kruif & Zhulina, 1996; Horne, 2006). Moreover, the porous and open structure of CM due to the high proline content provides an excellent release mechanism for bioactive delivery in the stomach (Fox, 2003; Livney, 2010). Consequently, CM can be an excellent matrix to carry hydrophobic molecules and other biopolymers (Ranadheera et al., 2016). Caseins without a well-defined permanent second or tertiary structure have been described as rheomorphic (Holt & Sawyer, 1993) meaning that they may adapt their structure to suit various conditions. CM structure is therefore not steady since several structural

modifications can occur and even lead to the disruption of the CM framework due to changes of physico-chemical parameters such as pH, ionic strength, water activity, temperature or pressure (De La Fuente, 1998; Gaucheron, 2005). However, CM structural stability can be improved by intra-micellar cross-linking using transglutaminase enzyme (TGase) to form strengthened structures called casein nanogel particles (De Kruif, Huppertz, Urban, & Petukhov, 2012; Huppertz & de Kruif, 2008; Smiddy, Martin, Kelly, de Kruif, & Huppertz, 2006).

TGase has several applications in food processing aiming to enhance functional properties of proteins (Romeih & Walker, 2017; Yokoyama, Nio, & Kikuchi, 2004) by catalyzing covalent binding between protein-bound glutaminyl side chain and protein-bound lysyl side chain (Motoki, Seguro, Nio, & Takinami, 1986). It has been clearly shown that TGase cross-linking increases the stability of CM against dissociating agents (Smiddy et al., 2006), ethanol coagulation (Huppertz & De Kruif, 2007a) and heat treatment (O'Sullivan, Kelly, & Fox, 2002). Particularly, many studies have focused on the major gel property modifications obtained from TGase cross-linked CM (Ardelean, Jaros, & Rohm, 2013; Jaros, Jacob, Otto, & Rohm, 2010; Lorenzen, Neve, Mautner, & Schlimme, 2002). However, up to now, the topographical and nanomechanical properties of individual TG-CM have never been investigated.

The aim of the present research is to evaluate the morphology and nanomechanics of TGase cross-linked CM (TG-CM) using atomic force microscopy (AFM) in lactose-free simulated milk ultrafiltrate (SMUF, pH 6.6) to replicate the native mineral environment of CM (Jenness & Koops, 1962). This technique provides soft material evaluation with minimal sample preparation to preserve its native properties (Jiao & Scha, 2004; Kasas, Longo, & Dietler, 2013). Nevertheless, AFM requires the immobilization of samples on a flat surface prior to study. In this work, CM and TG-CM were captured before AFM by weak interactions via a

specific MAH-PSer/Thr/Tyr antibody covalently bound to a carboxylic acid self-assembled monolayer on a gold surface. This capture method was previously developed and tested on native casein micelles (Bahri et al., 2017). The characterization of TG-CM, individual internal cross-linked casein micelle, was carried out in parallel with that of native CM and was also intended to validate the sensitivity of this methodology to investigate the topographical and nanomechanical properties of casein micelles.

2. Material and methods

2.1. Reagents

Tri-potassium citrate, tri-sodium citrate, KH_2PO_4, K_2SO_4 were purchased from Alfa Aesar (Heysham, UK). K_2CO_3 and $CaCl_2$ were from Amresco (Solon, Ohio, USA) and acetic acid, $MgCl_2$, KCl and KOH from VWR BDH Prolabo (Fontenay-sous-bois, France). 11-mercapto-1-undecanoic acid (11-MUA), N-ethyl-dimethylaminopropylcarbodiimide (EDC), N-hydroxysuccinimide (NHS) and sodium azide were obtained from Sigma-Aldrich (Saint-Quentin Fallavier, France). Sodium acetate was purchased from Merck (Darmstadt, Germany). Transglutaminase (TGase, Activa WM®) was a gift from Ajinomoto Foods Europe S.A.S. (Mesnil-Saint-Nicaise, France). Mouse anti-human phospho-Ser/Thr/Tyr monoclonal antibody (MAH-PSer/Thr/Tyr antibody) was from Spring Bioscience (E3074 - Pleasanton, CA, USA). HBS-N buffer (0.01 M HEPES, 0.15 M NaCl, pH 7.4) and ethanolamine hydrochloride 1 M pH 8.5 were purchased from Biacore (GE Healthcare, Velizy-Villacoublay, France). All solutions were prepared using Milli-Q water (Millipore®).

2.2. Preparation of native and cross-linked casein micelle dispersions

Native phosphocasein (PC) powder purchased from Ingredia SA (Promilk 852B, lot 131088, Arras, France) has been industrially obtained by microfiltration and diafiltration using the

milk mineral soluble phase ensuring a quasi-native state to the prepared casein micelles. PC powder contained 95 g dry solids per 100 g of powder and, in dry basis (w/w), 86% total proteins (corresponding to 79.1% caseins).

Casein micelle dispersion (5%, w/w) was prepared by dissolving PC powder in pH 6.6 lactose-free simulated milk ultrafiltrate (SMUF), replicating the mineral environment of native CM (Jenness & Koops, 1962). The dispersion was stirred at 540 rpm for 30 min at 20 °C before being stored overnight at 4 °C improving powder hydration. The PC dispersion was then warmed at 40 °C for 1 h and rapidly cooled to 20 °C just before experiments to ensure complete equilibration. To prevent microbial growth, sodium azide (0.35 g/L) was added to all samples.

CM cross-linked by TGase (TG-CM) were obtained from PC dispersion prepared as described above, equilibrated at 30 °C for 2 h and then incubated with 0.5 g/L TGase (100 U/g activity) at 30 °C for 24 h. Then, TGase was inactivated by heating the dispersion at 70 °C for 10 min, followed by a rapid cooling to room temperature in an ice-water bath (Smiddy et al., 2006). The cross-linkage of CM by TGase was checked by investigating the CM demineralization by sodium citrate addition up to 100 mmol.L^{-1} and turbidity measurements at 633 nm (Huppertz, Smiddy, & de Kruif, 2007) as shown in Table S1. A PC control dispersion was concurrently prepared following the same thermal history as TG-CM but without addition of TGase.

2.3. Micelle size distribution by photon correlation spectroscopy

The CM size distribution was evaluated by photon correlation spectroscopy (PCS) using a Zetasizer Nano-ZS equipment (Malvern Instruments, Malvern, UK) at 25 °C. Before analyses, each sample was diluted 20-fold with SMUF to avoid multiple diffusion phenomena during PCS measurement. Experimental data were assessed by the NNLS algorithm with the

dispersant viscosity taken as 0.89 mPa.s and the refractive index as 1.33 at 25 °C. Characteristics of the dispersed CM particles were taken as for milk proteins: 0.004 and 1.36 for the imaginary and the real refractive indices, respectively (Regnault, Thiebaud, Dumay, & Cheftel, 2004). For each independent sample, a mean distribution curve in intensity and in number was calculated from six measurements as well as the mean diameter (arithmetical mean).

2.4. Scanning electron microscopy (SEM)

Scanning electron microscopy (SEM) was used to evaluate CM shape. SEM samples were prepared as described in a previous work (Gastaldi, Lagaude, & De La Fuente, 1996). Briefly, ANODISC® membranes (Whatman, Maidstone, England) with an average pore diameter of 200 nm were immersed overnight in CM dispersion. After dehydration in a series of graded ethanol solutions (25-100%), the specimens were dried using a critical point dryer (Bal-Tec AG, Balzers, Liechtenstein, Germany). Then, the patterns were sputtered with gold palladium and analyzed with a Hitachi S-4800 scanning electron microscope at an accelerating voltage of 2 kV.

2.5. Atomic force microscopy

2.5.1. CM capture for AFM experiment

CM were captured by low energy interactions via MAH-PSer/Thr/Tyr antibody as described in a previous work (Bahri et al., 2017). All immobilization steps were carried out at room temperature. As a first step, a gold-sputtered glass chip (AU.0500.ALSI, Platypus Technologies LLC, Madison, WI, USA) was chemically cleaned twice with piranha solution (70% H_2SO_4 plus 30% H_2O_2), then three times with ethanol. The cleaned chip was immediately immersed in an ethanolic solution of 11-MUA (5 mM) for 18 h to coat the

surface with a self-assembled monolayer (SAM) of carboxyl groups. The chip was then extensively rinsed with absolute ethanol and ultrapure water before being immersed for 1 h in a MAH-PSer/Thr/Tyr antibody solution (50 µg/mL) prepared in acetate buffer (10 mM, pH 5). It was rinsed with acetate buffer (10 mM, pH 5), then with HBS-N buffer (0.01 M HEPES, 0.15 M NaCl, pH 7.4) before immersion into ethanolamine solution (1 M, pH 8) for 30 min to block free binding sites. The prepared chip was then immediately immersed into the TG-CM dispersion for 1 h, rinsed with SMUF and equilibrated for 4 h at room temperature before AFM measurements.

2.5.2. AFM measurements

The AFM experimental system used was an Asylum MFP-3D head coupled to the Molecular Force Probe 3D controller (Asylum Research, Santa Barbara, CA, USA). The microscope was placed in an acoustic isolation enclosure with an anti-vibration system. Silicon nitride cantilevers MLCT were purchased from Veeco Metrology Group (Santa Barbara, CA, USA), with a nominal spring constant of 0.01 $N.m^{-1}$ and an half-opening angle of 35°. Prior to each experiment, the cantilever spring constant was determined in liquid environment using the thermal noise method included in the MFP-3D software. AFM height, deflection trace and retrace topographic images, with a pixel resolution of 256 pixels at a line rate of 0.6 Hz, were obtained in contact mode in SMUF at room temperature. After testing a range of loading forces on different individual TG-CM, measurements were performed with a maximum loading force of ~100 pN. Higher loading force values led to stiffness overestimation due to the substrate. It was particularly checked that CM and TG-CM retained the same spherical cap section shape and remained adhered before and after indentation experiments (Figure S1). A constant approach velocity of 6 $\mu m.s^{-1}$ was used, meaning a piezo-extension rate of 3 Hz to minimize hydrodynamic and viscoelastic artifacts (Rosenbluth, Lam, & Fletcher, 2006).

The height (h) and width (w) distributions were obtained from the single TG-CM size analysis using the MFP-3D software. The contact angle (θ) of each TG-CM was deduced from the AFM-measured height and width using the equation (1):

$$\theta = 180 \text{ Arccos } (1- (h/w)) /\pi \qquad (1)$$

The elastic deformation was obtained from the force curves as a function of the loading force applied by the tip. The Young's modulus (E) was calculated for each force curve from the approaching part of the curve according to a modified Hertz model (Hertz, 1881), as described by Martin et al. (2013).

Experiments were repeated 3 times on different AFM gold chips.

2.5.3. AFM data analysis

Raw images were corrected by an implemented Asylum software using a standard procedure (flatten, planefit and artifact lines caused by the tip attachement and removal). Longitudinal profiles at selected zones were also obtained by the software. The scale indicating the sample height or deflection was adjusted to limit the gap between high and low regions. The individual elasticity values for a sample were collected via the Asylum software providing the distribution of elasticity values. Counts were normalized considering the total collected elasticity values of the specimen. A Gaussian fitting was then applied using the multi-peak analyzing software implemented in the MFP-3D operating system and OriginPro 8 software.

2.6. Statistics

Results were expressed as mean ± standard deviation. All the AFM and PCS results were analyzed by the Student's t-test. Statistical significance was set at $p < 0.05$.

3. Results and discussion

3.1. Topography of transglutamisase cross-linked CM

The influence of TG cross-linking has been evaluated on the apparent CM shape and dimensions. Fig. 1a-h shows AFM height and deflection images of CM and TG cross-linked CM captured on SAM-gold substrate via MAH-PSer/Thr/Tyr antibody when imaged in contact mode under native conditions (SMUF, pH 6.6). Scan parameters were adjusted for optimum contrast and stability and no lateral displacement of particles was recorded during analyses. These images (Fig. 1a-h) emphasize the efficiency of specific antibody capture of TG-CM that reveal a spherical cap shape, as already observed for native CM (Bahri et al., 2017). The native CM and TG-CM surface appears topographically homogeneous. This observation was confirmed by SEM micrographs (Fig. 2), which display different-sized CM and TG-CM (range of 40-300 nm) with a typical spherical shape and a rough surface. Moreover, SEM images of TG-CM (Fig. 2b, d) do not show the presence of CM aggregates proving that TGase cross-linking is exclusively intra-micellar.

According to the 2D and 3D AFM heights (Fig. 1a, c, e, g, h, j, l), it appeared that TG-CM are higher and wider than native CM. The surface coverage of TG-CM (11 ± 4 micelles/μm^2) was significantly ($p < 0.05$) lower than the native CM surface coverage (20 ± 2 micelles/μm^2), this lower density being attributed to the smaller size of native CM compared to TG-CM. At the same time, the hydrodynamic diameter distribution curves of native CM and TG-CM measured by PCS have been compared. The both size distribution curves in intensity exhibit monomodal and polydisperse populations (Fig. 3). TG-CM have however a significantly ($p < 0.05$) higher average hydrodynamic diameter of 214 ± 8 nm compared to 192 ± 8 nm for native CM.

This result was confirmed by the height and width distributions (Fig. 4a, b) obtained from the single TG-CM size analysis using the MFP-3D software. All in all, 250 features obtained from 10 different 2D-AFM images were analyzed. The size counts were normalized

considering the total collected values of samples. A multi-peak fitting was then applied using OriginPro 8 software to calculate the mean width and height. As depicted in Fig. 4a, b, TG-CM are polydisperse with monomodal width and height distributions and they are significantly ($p < 0.05$) wider (264 ± 7 nm) and higher (111 ± 5 nm) than native CM investigated in the same conditions and characterized by a mean width of 148 ± 8 nm and a mean height of 42 ± 1 nm (Bahri et al., 2017).

The morphological AFM results as those from SEM strongly show that TGase cross-linking is intra- and not inter-micellar, which is in good agreement with previous studies that underlined the intra-micellar cross-linking of native CM using different methods such as PCS, SLS and SAXS (Huppertz & De Kruif, 2008). However, it has been until now mentioned that CM size was not modified by TGase cross-linking. Nevertheless, the present results obtained from AFM and PCS data indicate that TGase cross-linking increases CM size as also observed previously on covalently cross-linked CM using genipin (Nogueira Silva, Bahri, Guyomarc'h, Beaucher, & Gaucheron, 2015). On the other hand, from SEM images (Fig. 2), the size difference between native CM and TG-CM was not clearly observable. This phenomenon could be attributed to CM shrinkage caused by the critical point drying of samples during the preparation steps since CM are highly hydrated features and therefore, drying process has an important impact on micellar structure. These observations are in accordance with other studies reporting distortion of CM particles due to the drying step during sample preparation for SEM (Dalgleish, Spagnuolo, & Goff, 2004; Martin, Goff, Smith, & Dalgleish, 2006; McMahon & Oommen, 2008).

AFM size characteristics were used to calculate the native CM and TG-CM volume; it should remain constant even after particle adsorption upon the surface (Evangelopoulos, Glynos, & Koutsos, 2012). The volume of the TG-CM was then calculated using MFP-3D software by performing the sum of all the heights of the micelle multiplied by the X scale and Y scale.

TG-CM have a volume of ~ 5x 10^6 nm^3 that higher than that measured for native CM (~ 1 x 10^6 nm^3), leading to a mean diameter of 214 nm for TG-CM and 123 nm for native CM considering CM as spherical. These values are consistent with the hydrodynamic diameter obtained by PCS for TG-CM.

Height and width distributions (Fig. 4a, b) show that TG-CM captured on SAM-gold substrate via MAH-PSer/Thr/Tyr antibody were definitely larger than higher, as it was also the case for native CM (Bahri et al., 2017). According to AFM size data, native CM and TG-CM have the shape of a spherical cap section rather than a sphere. This deformation, attributed to the adsorption upon gold substrate, can be evaluated by the ratio calculation between height and width, the perfect spherical particle width being equal to its height (h/w ~ 1). TG-CM data reveal a h/w ratio of ~ 0.5 higher than the native CM ratio (~ 0.3), indicating that native CM have a flatter shape compared to TG-CM. A previous study also evaluated the h/w ratio equal to 0.3 for native CM in liquid conditions and also highlighted CM deformation due to attachment on the substrate without losing volume in the case of CM immobilization on gold substrate via amine-coupling strategy (Ouanezar, Guyomarc'h, & Bouchoux, 2012). The h/w ratio of native CM and TG-CM implies a liquid droplet like behavior (Helstad et al., 2007). This deformation can also be displayed by plotting the height against the width for each single object (Fig. 4c, d). The comparison with the dotted line representing a perfect sphere points towards the fact that the TG-CM (Fig. 4c) are less flattened compared to native CM (Fig. 4d) once captured on the gold substrate. This phenomenon clearly highlights a structural strengthening of CM due to the molecular rearrangements induced by TGase.

The CM contact angle was deduced from the AFM-measured (h and w) of each CM. The contact angle (θ) corresponding to the interior angle formed by the substrate and the tangent to the drop interface at the apparent intersection of these interfaces describes the object deformation upon adsorption (Brown, 1999; Russel, 2009). A small contact angle is observed

when the particle spreads on the surface, while a large contact angle is observed when the liquid beads on the surface. More specifically, a perfect spherical particle would exhibit a contact angle greater than 90° (Yuehua & Randall, 2013). The equilibrium shape of a given particle does not depend only on surface forces but is also greatly affected by the elastic modulus of the droplet, the droplet deformation depending of material elastic nature resulting from stress development across the bulk in opposition to that deformation (Brown, 1999; Evangelopoulos et al., 2012). According to the AFM data analysis, TG-CM have a contact angle θ of 62° against the coated surface. Conversely, native CM have a significantly ($p < 0.05$) lower contact angle value of 44°. These results confirm the observed less deformation of TG-CM than native CM after capture on gold substrate.

An important change of the CM topography and elastic properties occurred after CM cross-linking with TGase compared to native CM. Cross-linked CM were significantly higher and larger than native CM pointing towards significant modifications in the CM structure due to TG crosslinking. A previous study highlighted a similar effect on CM height after crosslinking with genipin by AFM measurements in air, but widths were narrower probably due to dry condition (Nogueira Silva et al., 2015). Unlike control native CM, TG-CM were less deformed when adsorbed on gold substrate as reflected by a higher contact angle. Depending strongly on object elasticity, this high contact angle value revealed the harder aspect of TG-CM compared to native CM. The ratio h/w confirmed this observation since it was higher than that evaluated for native CM.

3.2. Nanomechanical properties of TG-CM

To explore nanomechanical properties of CM, low indenting forces were applied on each individual micellar object. CM kept the same shape and neither displacement nor disintegration was recorded after indentation experiments. A low loading force value of ~ 100

pN was chosen for nanoindentation to avoid CM damage due to the AFM tip and ensure a minimal deformation in the CM-substrate region. Ten force curves were applied at the center of each individual CM. The elasticity of CM at a given position was then calculated by fitting the approach part of the force curve using the Hertz model (Hertz, 1881; Uricanu, Duits, & Mellema, 2004) (Figure S2). In order to confirm the position of the analyzed particles, successive images were regularly performed and compared (Figure S1). Furthermore, by reducing the indentation to 20 nm, the contribution of the hard substrate on the calculated elasticity value was minimized. The elasticity of 20 micellar objects was calculated to obtain about 200 elasticity values.

The histogram of TG-CM stiffness values (Fig. 5) reveals a multimodal stiffness distribution with three prominent peaks at 218 ± 14 kPa, 536 ± 10 kPa and 711 ± 11 kPa, as identified by the peak analyzing software. The intensity of the three Gaussian distributions used to fit the TG-CM histogram is similar suggesting that the three populations have the same weight (Fig. 5). In comparison, a broad unimodal stiffness distribution with a peak centered at 269 ± 14 kPa was observed for native immobilized CM (Fig. 5). Generally, the mechanical heterogeneity of apparent Young's moduli is attributed to the complexity of the CM structure, the AFM tip indenting different components of the outer layer or of the core of CM (Bahri et al., 2017). Actually, hydrophobic bonds, negatively charged surface and calcium phosphate nanoclusters are involved in this complexity. In the case of TG-CM, the softest stiffness peak value (218 ± 14 kPa) is comparable to native CM Young's modulus value (269 kPa ± 14 kPa), and presumably represents a population with characteristics close to those of native CM. The two other stiffer peaks (535 ± 10 kPa and 710 ± 11 kPa) were most likely due to substantial changes in the shape and structure of CM induced by the TGase activity, as suggested by the size and topographical AFM data. This modification could be attributed to the creation of new casein dimers and oligomers formed by crosslinking peptide bound glutamine and lysine

residues after incubation with TGase (Ardelean et al., 2013; Smiddy et al., 2006). It is demonstrated that TGase creates intramicellar bonds; hence, κ-casein which is placed on the surface of the CM is the most involved in the polymerization reaction started by TGase followed by β and α_s casein, respectively (Ardelean et al., 2013; Huppertz & de Kruif, 2007a, 2007b; Jaros et al., 2010; Sharma, Lorenzen, & Qvist, 2001). This is probably related to the respective locations of caseins within the CM since CM is recognized as complex network of caseins chains with κ-casein hairy layer predominately present on the surface while β-casein is mostly present in the interior and α_s-casein is located all over the structure (Dalgleish & Corredig, 2012; De Kruif & Holt, 2003; Marchin, Putaux, Pignon, & Léonil, 2007).

To date, there are very few studies in literature on the effect of TGase cross-linking on the elasticity of individual CM at nanoscopic scale. Nieuwland, Bouwman, Bennink, Silletti, & de Jongh (2015) investigated the elastic modulus of individual CM cross-linked by TGase at different concentrations (0 to 90 U/g) using the Derjaguin, Muller, Toporov model applied on AFM force curves. The maximum modulus was observed for the highest TGase concentration, slightly lower than the TGase concentration fixed in this study. This is in accordance with the present results since the stiffness distribution of TG-CM was characterized by two peaks (536 ± 10 kPa and 711 ± 11 kPa) stiffer than the native CM Young's modulus value (269 kPa ± 14 kPa).

At macroscopic scale, the cross-linked TG-CM have been investigated focusing on TG-CM gelling properties by rheological measurements, highlighting an increase in stiffness and breaking strain of the TG-CM acid gels (Anema, Lauber, Lee, Henle, & Klostermeyer, 2005; Faergemand & Qvist, 1997; Faergemand, Sorensen, Jorgensen, Budolfsen, & Qvist, 1999; Lauber, Henle, & Klostermeyer, 2000). The gel microstructure modification observed in these studies at the macroscopic scale is attributed to the introduction of new covalent bonds in individual CM. This resulted at nanoscale in a higher stiffness of individual TG-CM

compared to native CM as shown by AFM nanomechanical characterization indicating that TGase modified the nanoscale organization of CM from colloids association to microgel particles.

Besides, these AFM results on the nano-structural properties of individual CM after enzymatic cross-linking highlight significant modifications probably inducing changes in the functional properties of caseins.

Conclusions

In summary, this study of TG-CM by AFM in liquid environment presents the first investigation on the size and nanomechanical properties of individual TG-CM. The AFM 2D images reveal a spherical–cap shape with a wider (264 ± 7 nm) and higher (111 ± 5 nm) structure than native CM. Moreover, TG-CM shows a more resistant structure upon adsorption on gold substrate owing to a high contact angle of 62°.

The TG-CM nanomechanical properties highlight a low elasticity peak at 218 ± 14 kPa that could correspond to the mechanical signature of native CM and also two stiffer elasticity peaks observed at 536 ± 10 kPa and 711 ± 11 kPa, most likely directly related to substantial changes in the shape and structure of CM induced by TGase and responsible for the modification of their functional properties.

These results support the improved stability of TG-CM suggesting that these nanogel particles can be an excellent matrix for bioactives encapsulation.

Acknowledgements

We thank the French Ministry of Higher Education and Research for financial support and M. D. COT from the European Institute of Membrane, Montpellier, France for the SEM analysis.

Transglutaminase Activa® WM was kindly provided by Ajinomoto Foods Europe S.A.S (Mesnil-Saint-Nicaise, France).

References

Anema, S. G., Lauber, S., Lee, S. K., Henle, T., & Klostermeyer, H. (2005). Rheological properties of acid gels prepared from pressure- and transglutaminase-treated skim milk. *Food Hydrocolloids*, *19*(5), 879–887.

Ardelean, A. I., Jaros, D., & Rohm, H. (2013). Influence of microbial transglutaminase cross-linking on gelation kinetics and texture of acid gels made from whole goats and cows milk. *Dairy Science and Technology*, *93*(1), 63–71.

Bahri, A., Martin, M., Gergely, C., Pugnière, M., Chevalier-Lucia, D., & Marchesseau, S. (2017). Atomic force microscopy study of the topography and nanomechanics of casein micelles captured by an antibody. *Langmuir, 33(19)*, 4720–4728.

Brown, R. (1999). *Handbook of polymer testing* (Marcel Dek). New York.

Chevalier-Lucia, D., Blayo, C., Grácia-Juliá, A., Picart-Palmade, L., & Dumay, E. (2011). Processing of phosphocasein dispersions by dynamic high pressure: Effects on the dispersion physico-chemical characteristics and the binding of α-tocopherol acetate to casein micelles. *Innovative Food Science and Emerging Technologies*, *12*(4), 416–425.

Dalgleish, D. G., & Corredig, M. (2012). The structure of the casein micelle of milk and Its changes during processing. *Annual Review of Food Science and Technology*, *3*, 449–467.

Dalgleish, D., Horne, D. S., & Law, A. J. R. (1989). Size-related differences in bovine casein micelles. *Biochemica et Biophysica Acta*, *991*, 383–387.

Dalgleish, D. G., Spagnuolo, P. A., & Goff, H.D. (2004). A possible structure of the casein micelle based on high-resolution field-emission scanning electron microscopy. *International Dairy Journal*, *14*, 1025–1031.

De Kruif, C. G., & Holt, C. (2003). Casein micelle structure, functions and interactions. *Advanced Dairy Chemistry*, *1*(3), 233–275.

De Kruif, C. G., & Zhulina, E. B. (1996). κ-Casein as a polyelectrolyte brush on the surface of casein micelles. *Colloids and Surfaces A: Physicochemical and Engineering Aspects*, *117*(1–2), 151–159.

De Kruif, C. G., Huppertz, T., Urban, V. S., & Petukhov, A. V. (2012). Casein micelles and their internal structure. *Advances in Colloid and Interface Science*, *171–172*, 36–52.

De La Fuente, M. A. (1998). Changes in the mineral balance of milk submitted to technological treatments. *Trends in Food Science and Technology*, *9*(7), 281–288.

Evangelopoulos, A. E. A. S., Glynos, E., & Koutsos, V. (2012). Elastic Modulus of a Polymer Nanodroplet : Theory and Experiment. *Langmuir*, *10*(28), 4754–4767.

Faergemand, M., & Qvist, K. B. (1997). Transglutaminase: effect on rheological properties, microstructure and permeability of set style acid skim milk gel. *Food Hydrocolloids*, *11*(3), 287–292.

Faergemand, M., Sorensen, M., Jorgensen, U., Budolfsen, G., & Qvist, K. (1999). Transglutaminase: effect on instrumental and sensory texture of set style yoghurt. *Milchwissenschaft-Milk Science International*, *54*, 563–566.

Fox, P. F. (2003). Milk proteins: general and historical aspects. In P. F. Fox & P. L. H. McSweeney (Eds.), *Advanced Dairy Chemistry: volume 1: Proteins, Parts A&B* (pp. 1–48). Springer US.

Gastaldi, E., Lagaude, A., & De La Fuente, B. T. (1996). Micellar transition state in casein between pH 5.5 and 5.0. *Journal of Food Science*, *61*(1), 59–64.

Gaucheron, F. (2005). The minerals of milk. *Reproduction, Nutrition, Development*, *45*, 473–483.

Helstad, K., Rayner, M., Van Vliet, T., Paulsson, M., & Dejmek, P. (2007). Liquid droplet-

like behaviour of whole casein aggregates adsorbed on graphite studied by nanoindentation with AFM. *Food Hydrocolloids*, *21*(5–6), 726–738.

Hertz, H. (1881). Über die Berührung fester elastischer Körper. *Journal Für Die Reine Und Angewandte Mathematik*, *92*, 156–171.

Holt, C., & Sawyer, L. (1993). Caseins as rheomorphic proteins: interpretation of primary and secondary structures of the αs1-, β- and κ-caseins. *Journal of the Chemical Society, Faraday Transactions*, *89*(15), 2683–2692.

Horne, D. S. (2006). Casein micelle structure: Models and muddles. *Current Opinion in Colloid & Interface Science*, *11*(2–3), 148–153.

Huppertz, T., & de Kruif, C. G. (2007a). Ethanol stability of casein micelles cross-linked with transglutaminase. *International Dairy Journal*, *17*(5), 436–441.

Huppertz, T., & de Kruif, C. G. (2007b). Rennet-induced coagulation of enzymatically cross-linked casein micelles. *International Dairy Journal*, *17*(5), 442–447.

Huppertz, T., Smiddy, M. A., & de Kruif, C. G. (2007). Biocompatible micro-gel particles from cross-linked casein micelles. *Biomacromolecules*, *8*, 1300–1305.

Huppertz, T., & de Kruif, C. G. (2008). Structure and stability of nanogel particles prepared by internal cross-linking of casein micelles. *International Dairy Journal*, *18*(5), 556–565.

Jenness, R., & Koops, J. (1962). Preparation and properties of a salt solution which simulates milk ultrafiltrate. *Netherlands Milk and Dairy Journal*, *16*, 153–164.

Jaros, D., Jacob, M., Otto, C., & Rohm, H. (2010). Excessive cross-linking of caseins by microbial transglutaminase and its impact on physical properties of acidified milk gels. *International Dairy Journal*, *20*(5), 321–327.

Jiao, Y., & Scha, T. E. (2004). Accurate height and volume measurements on soft samples with the atomic force microscope. *Langmuir*, *20*, 10038–10045.

Kasas, S., Longo, G., & Dietler, G. (2013). Mechanical properties of biological specimens

explored by atomic force microscopy. *Journal of Physics D-Applied Physics, 46,* 133001.

Katouzian, I., & Jafari, S.M. (2016). Nano-encapsulation as a promising approach for targeted delivery and controlled release of vitamins. *Trends in Food Science & Technology, 53,* 34–48.

Lauber, S., Henle, T., & Klostermeyer, H. (2000). Relationship between the crosslinking of caseins by transglutaminase and the gel strength of yoghurt. *European Food Research and Technology, 210,* 305–309.

Livney, Y. D. (2010). Milk proteins as vehicles for bioactives. *Current Opinion in Colloid and Interface Science*, *15*(1–2), 73–83.

Lorenzen, P., Neve, H., Mautner, A., & Schlimme, E. (2002). Effect of enzymatic cross-linking of milk proteins on functional properties of set-style yoghurt. *International Journal of Dairy Technology*, *55*(3), 152–157.

Marchin, S., Putaux, J. L., Pignon, F., & Léonil, J. (2007). Effects of the environmental factors on the casein micelle structure studied by cryo transmission electron microscopy and small-angle x-ray scattering/ultrasmall-angle x-ray scattering. *Journal of Chemical Physics*, *126*(4), 045101.

Martin, M., Benzina, O., Szabo, V., Végh, A. G., Lucas, O., Cloitre, T., Scamps, F., & Gergely, C. (2013). Morphology and nanomechanics of sensory neurons growth cones following peripheral nerve injury. *Plos One*, *8*(2), 1–11.

Martin, A. H., Goff, D. H., Smith, A., & Dalgleish, D. G. (2006). Immobilization of casein micelles for probing their structure and interactions with polysaccharides using scanning electron microscopy (SEM). *Food Hydrocolloids*, *20*(6), 817–824.

McMahon, D. J., & Brown, R. J. (1984). Composition, structure, and integrity of casein micelles: a review. *Journal of Dairy Science*, *67*, 499-512.

McMahon, D. J., & Oommen, B. S. (2008). Supramolecular structure of the casein micelle. *Journal of Dairy Science*, *91*(5), 1709–1721.

Motoki, M., Seguro, K., Nio, N., & Takinami, T. (1986). Glutamine-specific deamidation of αs1-casein by transglutaminase. *Agricultural and Biological Chemistry*, *50*(12), 3025–3030.

Nieuwland, M., Bouwman, W. G., Bennink, M. L., Silletti, E., & de Jongh, H. H. J. (2015). Characterizing length scales that determine the mechanical behavior of gels from crosslinked casein micelles. *Food Biophysics*, 10, 416-427.

Nogueira Silva, N. F., Bahri, A., Guyomarc'h, F., Beaucher, E., & Gaucheron, F. (2015). AFM study of casein micelles cross-linked by genepin: effects of acid pH and citrate. *Dairy Science and Technology*, *95*(1), 75–86.

O'Sullivan, M. M., Kelly, A. L., & Fox, P. F. (2002). Effect of transglutaminase on the heat stability of milk: A possible mechanism. *Journal of Dairy Science*, *85*(1), 1–7.

Ouanezar, M., Guyomarc'h, F., & Bouchoux, A. (2012). AFM imaging of milk casein micelles: evidence for structural rearrangement upon acidification. *Langmuir*, *28*, 4915–4919.

Prakash, V., & van Boekel, M. A. J. S. (2010). Nutraceuticals: possible future ingredients and food safety aspects. In C. E. Boisrobert, A. Sjepanovic, S. Oh, & H. L. M. Lelieveld (Eds.), *Ensuring Global Food Safety* (pp. 333–338). Oxford: University Press.

Ranadheera, C. S., Liyanaarachchi, W. S., Chandrapala, J., Dissanayake, M., & Vasiljevic, T. (2016). Utilizing unique properties of caseins and the casein micelle for delivery of sensitive food ingredients and bioactives. *Trends in Food Science and Technology*, *57*, 178–187.

Regnault, S., Thiebaud, M., Dumay, E., & Cheftel, J. C. (2004). Pressurisation of raw skim milk and of a dispersion of phosphocaseinate at 9 °C or 20 °C: Effects on casein micelle

size distribution. *International Dairy Journal*, *14*(1), 55–68.

Romeih, E., & Walker, G. (2017). Recent advances on microbial transglutaminase and dairy application. *Trends in Food Science and Technology*, *62*,133–140.

Rosenbluth, M. J., Lam, W. A., & Fletcher, D. A. (2006). Force microscopy of nonadherent cells : A comparison of leukemia cell deformability, *90*(1762), 2994–3003.

Russel, S. (2009). *Contact Angle Measurement Technique for Rough Surfaces*. Michigan Technological University.

Sharma, R., Lorenzen, P. C., & Qvist, K. B. (2001). Influence of transglutaminase treatment of skim milk on the formation of ε-(-glutamyl)lysine and the susceptibility of individual proteins towards crosslinking. *International Dairy Journal*, *11*(10), 785–793.

Smiddy, M. A., Martin, J.E. G. H., Kelly, A. L., de Kruif, C. G., & Huppertz, T. (2006). Stability of casein micelles cross-linked by transglutaminase. *Journal of Dairy Science*, *89*(6), 1906–14.

Uricanu, V. I., Duits, M. H. G., & Mellema, J. (2004). Hierarchical networks of casein proteins: An elasticity study based on atomic force microscopy. *Langmuir*, *20*(12), 5079–5090.

Walstra, P., Geurts, T. J., Noomen, A., Jellema, A., & van Boekel, M. A. J. S. (1999). Milk components. In P. Walstra, T. J. Geurts, A. Noomen, A. Jellema, & M. A. J. S. van Boekel (Eds.), *Dairy Technology* (pp. 27–105). New York: Marcel Dekker.

Yokoyama, K., Nio, N., & Kikuchi, Y. (2004). Properties and applications of microbial transglutaminase. *Applied Microbiology and Biotechnology*, *64*(4), 447–454.

Yuehua, Y., & Randall, L. (2013). Surface science techniques. In *Springer Series in Surface Sciences* (Vol. 51, pp. 3–34).

Zhu, F. (2017). Encapsulation and delivery of food ingredients using starch based systems. *Food Chemistry*, *229*, 542–552.

Figure captions

Figure 1: Native CM (a, b, e, f, i, j) and transglutaminase cross-linked CM (c, d, g, h, k, l) topography. AFM height (a, c, e, g) and deflection (b, d, f, h) images, height profile (i, k) at the selected black scan line on (e, g), three-dimensional AFM height image (j, l) of CM and TG-CM CM. CM and TG-CM were captured on SAM via MAH-PSer/Thr/Tyr antibody. Images were performed in liquid (SMUF, pH 6.6) in contact mode. The white scale bar (a-h) represents 1 µm. The colored scale bar (a, c, e, g) represents the height range between 0 and 120 nm. The grey scale bar (b, d, f, h) represents the deflection range between 0 and 30 nm.

Figure 2: SEM images of native CM (a, c) and transglutaminase cross-linked CM (b, d) on ANODISC® membrane at two different magnifications.

Figure 3: Particle size distribution curves of native (■) and TG cross-linked (•) CM (5%, w/w) determined by photon correlation spectroscopy (PCS) in light intensity. PCS measurements were carried out at 25 °C. Mean curves from six PCS determinations are shown.

Figure 4: Histograms of width (a) and height (b) and height versus width plots (c-d) for TG cross-linked (a, b, c) and native (d) CM. Height and width histograms were best fitted with a Gaussian function. The dotted lines in the height vs width plots show the linear ratio between width and height of a perfectly spherical particles.

Figure 5: AFM elasticity distribution indicating the stiffness of TG-CM in a liquid native environment (SMUF, pH 6.6). Young's modulus (E) distribution was best fitted with 3 Gaussian peaks centered at 218 ± 14 kPa, 536 ± 10 kPa and 711 ± 11 kPa (solid line).

564 Young's modulus distribution fit of native CM is proposed (dotted line) centered at 269 ± 14
565 kPa. 10 loading forces were applied on 20 different CM in order to obtain 200 analyzed
566 curves.

Figure 1

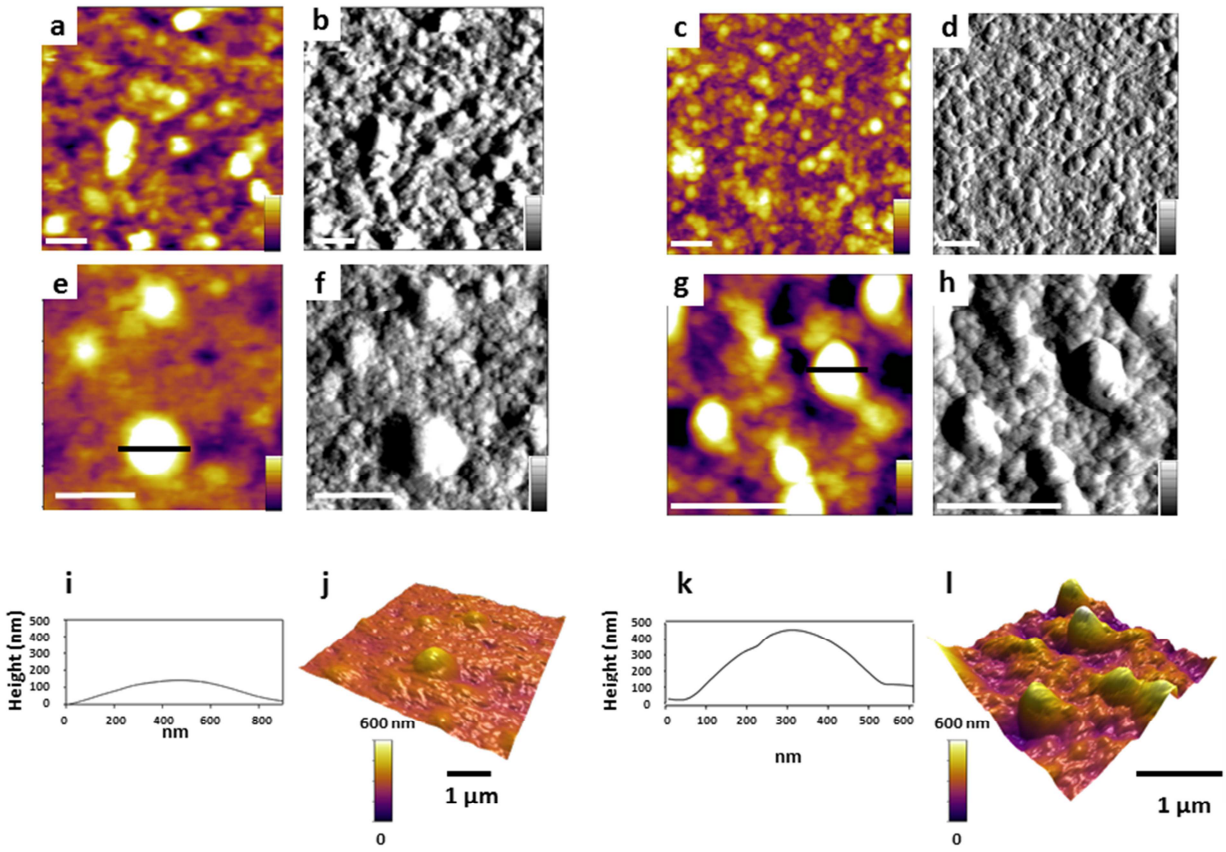

Comment citer ce document :
Bahri, A., Martin, M., Gergely, Marchesseau, S., Chevalier-Lucia, D. (2018). Topographical and nanomechanical characterization of casein nanogel particles using atomic force microscopy. Food Hydrocolloids, 83, 53-60. , DOI : 10.1016/j.foodhyd.2018.03.029

Figure 2

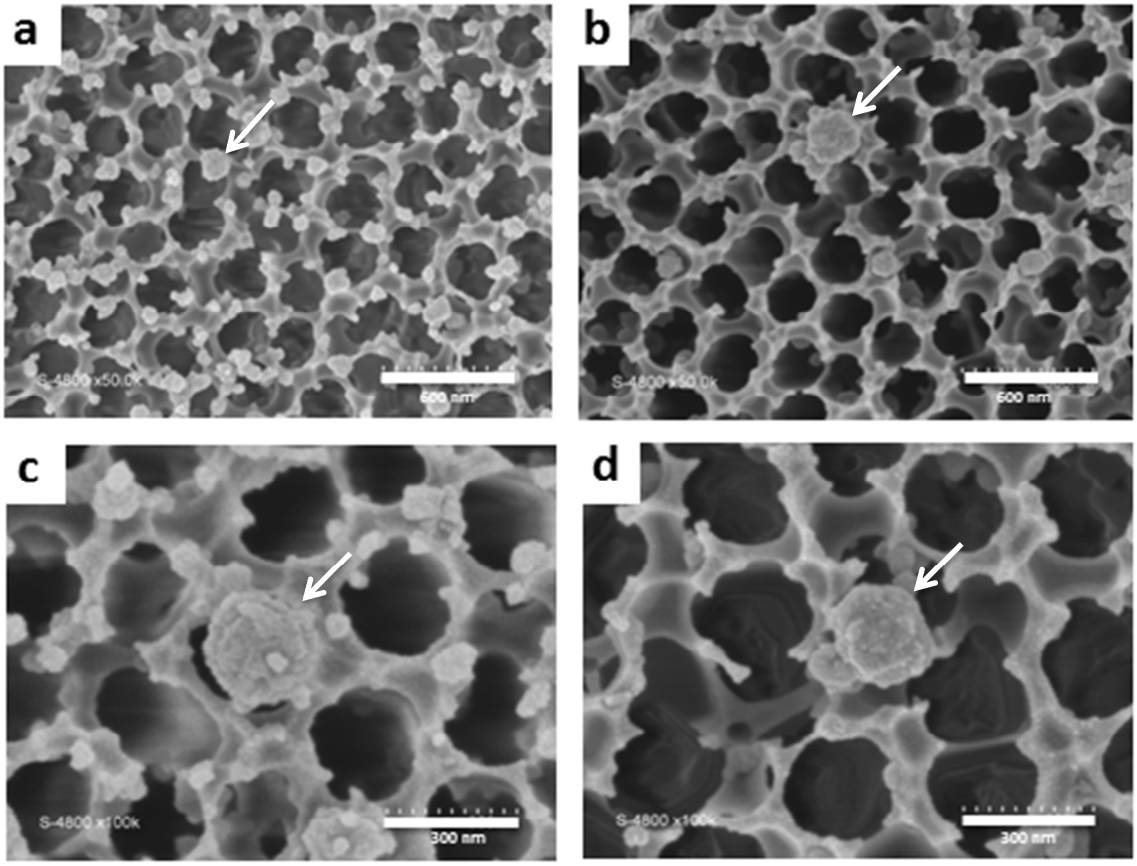

Comment citer ce document :
Bahri, A., Martin, M., Gergely, Marchesseau, S., Chevalier-Lucia, D. (2018). Topographical and nanomechanical characterization of casein nanogel particles using atomic force microscopy. Food Hydrocolloids, 83, 53-60. , DOI : 10.1016/j.foodhyd.2018.03.029

Figure 3

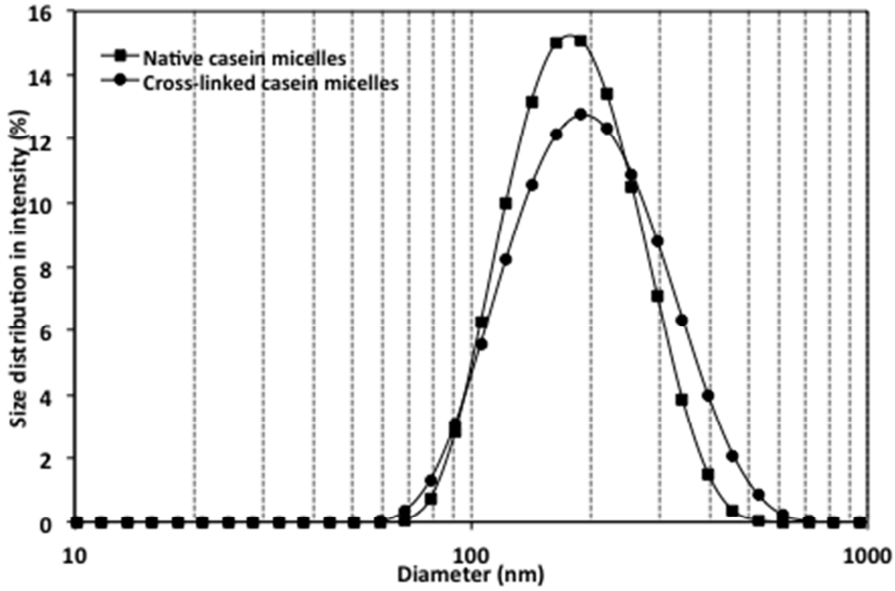

Comment citer ce document :
Bahri, A., Martin, M., Gergely, Marchesseau, S., Chevalier-Lucia, D. (2018). Topographical and nanomechanical characterization of casein nanogel particles using atomic force microscopy. Food Hydrocolloids, 83, 53-60. , DOI : 10.1016/j.foodhyd.2018.03.029

Figure 4

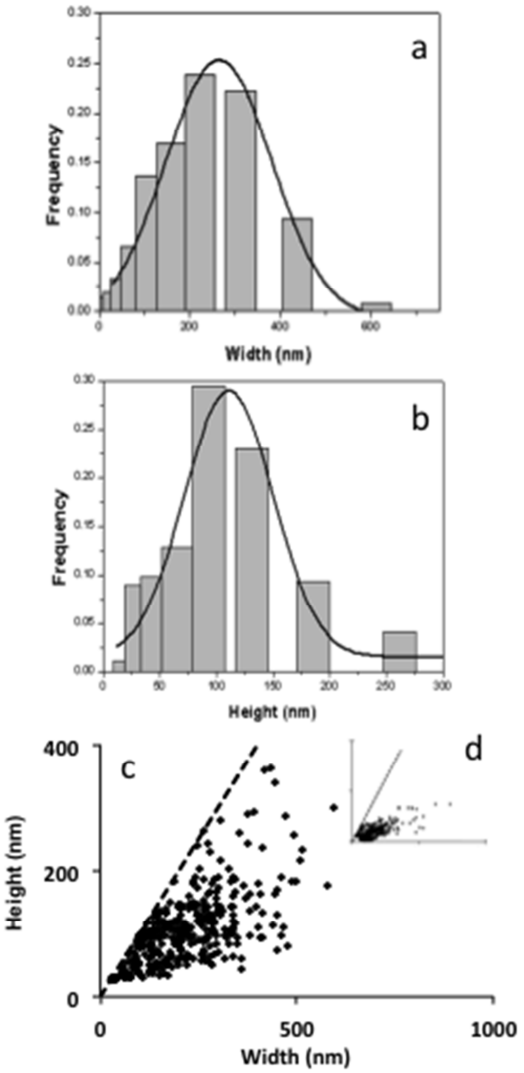

Figure 5

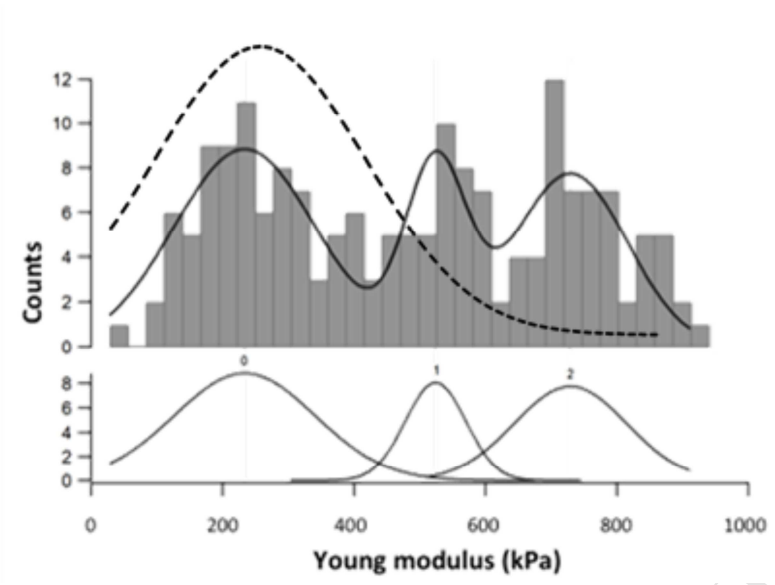

Highlights

- TG cross-linked CM topography and nanomechanics were evaluated by AFM in liquid.
- TG cross-linked CM are significantly wider and higher than native CM.
- TG-CM are less flattened once captured on gold substrate compared to native CM.
- TG-CM stiffness distribution is multimodal with stiffer peaks compared to native CM.